Virchows Arch (1996) 427:575–582

ORIGINAL ARTICLE

Robert Hume · Hazel Brewerton · Ann Burchell

The human embryonic-fetal kidney endoplasmic reticulum phosphate-pyrophosphate transport protein

Received: 16 October 1995 / Accepted: 12 December 1995

Abstract Glucose-6-phosphatase is a multicomponent endoplasmic reticulum system comprising at least six different proteins, including a lumenal enzyme and several transport proteins. One of the transport proteins, $T_2\beta$, transports the substrate pyrophosphate and the product phosphate and its genetic deficiency is termed type 1c glycogen storage disease. We have used anti-$T_2\beta$ antibodies for immunohistochemistry with image analysis and kinetic analysis of the glucose-6-phosphatase system to study for the temporal and spatial development of $T_2\beta$ in human embryonic and fetal kidney. In metanephric kidney, there is an early predominance of $T_2\beta$ expression in the ureteric bud derivatives and this changes with ontogeny such that developing nephrons, particularly proximal tubules, become dominant by mid-gestation. $T_2\beta$ has the same spatial and temporal pattern as the glucose-6-phosphatase enzyme in both mesonephric and metanephric kidney. Pyrophosphate transport capacity is appropriate for the amount of glucose-6-phosphatase activity present in mid-gestation fetal kidney, in contrast to liver, where pyrophosphate transport capacity is developmentally delayed. Increasing knowledge of the temporal and spatial expression of the glucose-6-phosphatase proteins and their catalytic roles in early human development is essential for the elucidation of the aetiology of renal disease in both type I glycogen storage diseases and the developmental disorders of the glucose-6-phosphatase system.

Key words Glucose-6-phosphatase · Endoplasmic reticulum · Phosphate transport · Pyrophosphate transport · Kidney

R. Hume (✉) · H. Brewerton · A. Burchell
Department of Obstetrics and Gynaecology, University of Dundee, Ninewells Hospital and Medical School, Dundee DD1 9SY, UK
Tel.: (44) 1382–66 01 11, ext. 2594; Fax: (44) 1382–56 66 17

R. Hume
Department of Child Health, University of Dundee, Dundee, UK

R. Hume
Department of Biochemical Medicine, University of Dundee, Dundee, UK

Introduction

The liver and, to a lesser extent, the kidney play a major role in regulation of blood glucose levels [25]. The two pathways by which they can make glucose are glycogenolysis and gluconeogenesis [24, 25]. One enzyme, microsomal glucose-6-phosphatase, catalyses the terminal step of both pathways [4, 6]. The importance of glucose-6-phosphatase in the regulation of blood glucose levels first became obvious in 1952 from the debilitating effects of the complete absence of the enzyme in type Ia glycogen storage disease [14, 17]. The genetic deficiencies of the glucose-6-phosphatase transport proteins for glucose-6-phosphate, phosphate and glucose are termed type 1b, 1c and 1d respectively [14]. Renal disease is now a well-recognised complication of type I glycogen storage disease (for recent review see [14]). It has also been suggested that in the kidney, glucose-6-phosphatase may play other roles, such as the regulation of calcium homeostasis in tubular cells [18] and in the transport of glucose across tubular cells, in addition to other established glucose transport mechanisms [24].

Liver glucose-6-phosphatase is a multicomponent system comprising at least six different proteins. These include the catalytic subunit of the glucose-6-phosphatase enzyme, which is situated on the lumenal side of the endoplasmic reticulum membrane and is associated with a regulatory calcium binding protein (Fig. 1A), [12]. In addition, there are at least four transport proteins, termed T_1 (or glucose-6-phosphate transport protein), $T_2\alpha$ and $T_2\beta$ (phosphate and pyrophosphate transport proteins) and T_3 (a glucose transport protein). All six proteins (Fig. 1) are required for normal glucose-6-phosphatase activity in vivo when glucose-6-phosphate is the substrate (Fig. 1B) [6]. Glucose-6-phosphatase will also hydrolyse a number of other substrates such as pyrophosphate and carbamyl phosphate and when pyrophosphate and carbamyl phosphate are the substrates, the only endoplasmic reticulum transport required is that of T_2 (Fig. 1C) [6, 26]. Recent studies in the liver have indicated that there are two different endoplasmic reticulum

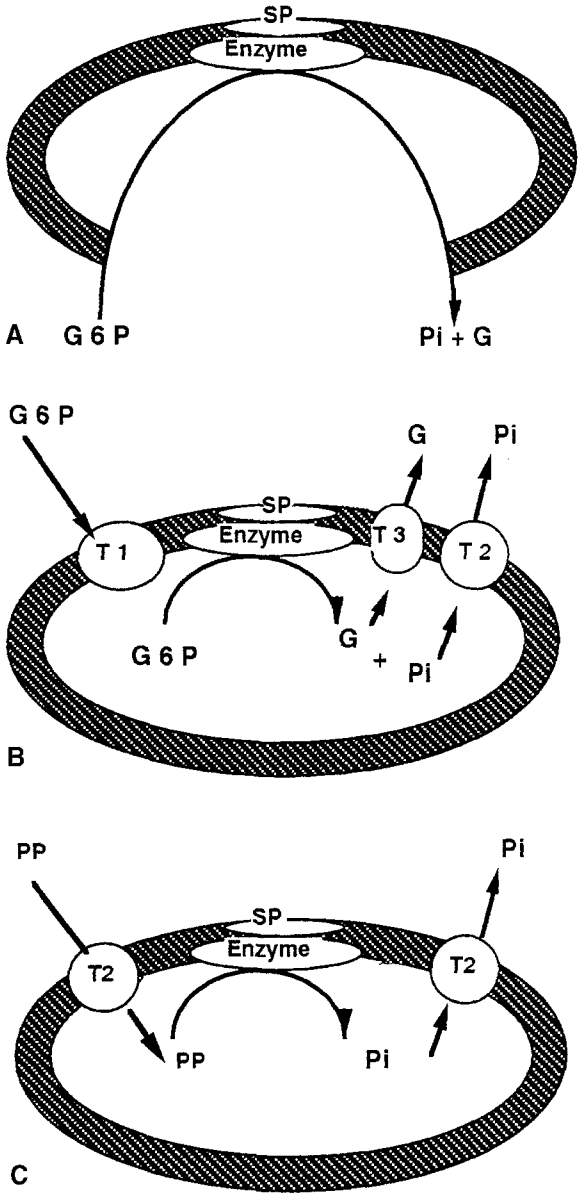

Fig. 1 Schematic representation of the proteins necessary for glucose-6-phosphatase activity **A** in fully disrupted microsomes, **B** in intact microsomes with glucose-6-phosphate as substrate, **C** in intact microsomes with pyrophosphate as substrate. (*T1* The microsomal glucose-6-phosphate transport protein, *T2* the microsomal phosphate and pyrophosphate transport proteins, *T3* the microsomal glucose transport protein, *Pi* inorganic phosphate, *SP* a regulatory Ca^{2+} binding protein, *Enzyme* the glucose-6-phosphatase enzyme, *G* glucose, *PP* pyrophosphate, *G6P* glucose-6-phosphate)

proteins capable of transporting phosphate. One of these, $T_2\beta$, also transports carbamyl phosphate and phosphate and its deficiency results in impaired glucose-6-phosphatase activity, i.e. type Ic glycogen storage disease [23, 26]. The hepatic microsomal glucose-6-phosphatase system has been characterised extensively in the last few years [6, 12] and recently, development of the glucose-6-phosphatase enzyme has been described in human kidney [21]. Little is known about the other components of the renal glucose-6-phosphatase system and nothing is known about kidney $T_2\beta$.

In normal term infants the activity of the liver glucose-6-phosphatase enzyme increases around 10-fold over the first 3 postnatal days [10], but in many preterm infants this developmental rise fails to occur with resultant impaired glucose homeostasis which may persist, certainly into childhood [19]. In addition, we have described three preterm infants who died and on analysis of hepatic autopsy samples, one was found to have abnormal glucose-6-phosphatase enzyme and two to have no $T_2\beta$ transport capacity [20]. In one of the $T_2\beta$-deficient infants, a renal autopsy sample showed $T_2\beta$ deficiency [20]. In view of the fact that we have subsequently shown that developmental disorders of this enzyme system are common [19], it is likely that these two cases of $T_2\beta$ deficiency have a developmental rather than genetic basis. The long-term renal consequences of $T_2\beta$ deficiency are likely to be similar, however, whether genetic or developmental in origin.

We have shown that in human fetal liver the development of $T_2\beta$ is delayed when compared with other components of the glucose-6-phosphatase system [10], but nothing is known of the temporal or spatial appearance of kidney $T_2\beta$ or whether $T_2\beta$ development in human kidney is similarly delayed.

Materials and methods

Chemicals

Glucose-6-phosphate (monosodium salt), mannose-6-phosphate (disodium salt) and histone type IIA and type II-AS were obtained from Sigma, Poole, UK. Sodium dodecyl sulphate (especially purified for biochemical work) and tetrasodium pyrophosphate were purchased from BDH, Poole, UK. Cacodylic acid was from Sigma and was recrystallised from 95% ethanol.

Tissue samples

Human embryonic tissue was obtained within 1 h following termination of pregnancies of less than 56 days amenorrhoea using Mifepristone (Roussel, Uxbridge, UK) and Gemeprost vaginal pessaries (May and Baker, Dagenham, UK). Stages of embryonic development and the approximate postovulatory days of age were established according to current morphological criteria [28]. Fetal tissue was obtained within 6 h following termination of pregnancy using Gemeprost vaginal pessaries. Fetal developmental age was carefully estimated based on size, including crown-heel, crown-rump and heel-toe measurements [33], menstrual history and ultrasound dating of pregnancy. Normality of fetuses was confirmed by autopsy. Adult and infant tissue was obtained at routine postmortem within 12 h of certification of death. The study was approved by the Paediatric Reproductive Medicine Ethics of Medical Research Sub-Committee of Lothian Health Board and the Ethics Committee of Tayside Health Board.

Tissue fixation and processing

Eight embryos (postovulatory age 32–56 days) were fixed in 10% buffered formalin for 5 days and processed routinely to paraffin wax. In a similar manner, kidneys were fixed and processed from nine fetuses (9–23 weeks' gestation), one spontaneous abortion at

27 weeks' gestation, two stillborn infants at 34 and 39 weeks' gestation. In addition kidneys from four fetuses 16–19 weeks' gestation were snap-frozen at –70°C.

Antibody

Monospecific polyclonal antisera to $T_2\beta$ was raised in a Cheviot sheep by three subcutaneous injections of 80 mg purified rat liver microsomal $T_2\beta$ protein [35] and Freund's complete adjuvant as previously described [7, 9]. Pre-immune serum was obtained prior to the injection with antigen. $T_2\beta$ protein used as antigen was isolated from starved Wistar rat hepatic microsomes. Antiserum was further purified by $(NH_4)_2SO_4$ fractionation and affinity purification using protein G columns and the resultant antibody preparation was used at protein concentrations described below. The antibody preparation, although raised against a rat liver protein, has been shown many times to cross-react well with the respective human proteins, e.g. [9, 26], as judged by immunoblot analysis following SDS PAGE.

Immunohistochemistry

Formalin-fixed, paraffin-embedded tissue was cut at 3-μm sections. The first section was stained with haematoxylin and eosin to confirm normality and developmental characteristics [31]. Immunohistochemistry was performed on sequential sections using the methods previously described in human liver, brain, kidney and adrenal [5, 11, 21, 22] with $T_2\beta$ antibody preparation diluted to 0.3 mg/ml. On further sections, negative controls were made by replacing each of the individual primary antibody preparations by non-immune serum. A standard peroxidase-antiperoxidase (PAP) technique was used incorporating 3,3-diaminobenzidine as developing agent [34] Sections were lightly counterstained with haematoxylin, dehydrated through graded alcohols, and cleared in xylene prior to coverslipping in synthetic resin.

Image analysis

The acquisition of light microscopic immunohistochemical images was made by a Zeiss microscope – JVC KYF 30-E 3 chip colour camera linked to an Apple Macintosh Quadra 950 computer, with a HR-24 RBG card (Improvision, University of Warwick) to allow capture of images up to 700×572 pixels in size and for control of the high-resolution monitor. Colourvision software (Improvision, University of Warwick) was used for video rate capture of 24-bit images with the ability to individually adjust red, green or blue threshold limits to allow thresholding and detection of different coloured populations. For precipitated 3,3-diaminobenzidine products on immunohistochemical sections, this was restricted to dark-brown staining (thresholds R1B1G1) monitored as a false red channel and medium-brown (thresholds R2B2G2) captured as a false green channel with analysis of the area occupied by each channel per total selected image area.

Sequential embryonic and fetal metanephric kidneys sections, made transversely through the hilum, were immunostained at the same time with the $T_2\beta$ antibody preparation. A series of image sections, 100×572 pixels, were sequentially captured across each of the stained kidney sections from the capsule to the pelvis. Individual image sections were then colour analysed, using the thesholds R1B1G1 and R2B2G2, and areas (pixels) of 3,3-diaminobenzidine product staining per total image section derived. The individual areas occupied by primitive glomerulo-tubular complexes, glomeruli, proximal tubules, distal tubules, loops of Henle, collecting ducts and papillary ducts of Bellini epithelium were computed for each serial image and colour analysis of the total area for each component kidney structure from all the serial images was accumulated. A measure of the intensity of $T_2\beta$ immunostaining in each renal component was derived from the area (pixels) of immunostaining divided by the epithelial area (pixels) for each component.

Images and data were routinely stored on optical discs and images captured in Colourvision were transferred through Adobe Photoshop 1.0.7 prior to printing by a Kodak XL-7700 colour printer.

Microsomal preparation

Microsomes were prepared from 10% homogenates of ten human fetal kidney samples (15–25 weeks' gestation) in 0.25 M sucrose/5 mM Hepes (pH 7.4) by differential centrifugation as previously described [8].

Assays

Glucose-6-phosphatase, mannose-6-phosphatase and pyrophosphatase activities were assayed in both untreated and disrupted microsomes for up to 30 min and calculated [8] and results are expressed as nanomoles of substrate hydrolysed per minute per milligram of microsomal protein. All assays were linear with respect to incubation time. The concentrations of the substrate glucose-6-phosphate used to calculate the kinetic constants were 1.0, 1.4, 2.0, 2.6, 5.0 and 30 mM and 0.5, 1.0, 1.4, 2.0, 2.6 and 5.0 mM were the concentrations of pyrophosphate used as a substrate. All V_{max} and K_m values given in this paper were calculated using a BBC computer program of non-linear multiple regression analysis [16]. Microsomes isolated from kidney homogenates (untreated microsomes) are a mixture of intact and disrupted structures. The proportion of intact microsomes were determined in all preparations by assays of low K_m mannose-6-phosphatase activity which is only expressed in disrupted structures [2, 3]. All of the microsomal preparations used in this paper were more than 90% intact. We have previously shown that in microsomal preparations which are greater than 75% intact no significant proteolysis of endoplasmic reticulum proteins occurred [11]. Latency is defined as the percentage of activity in disrupted microsomes which is not expressed in intact microsomes. Protein concentrations were estimated by the method of Lowry as modified by Peterson [30].

Results

Immunohistochemistry

Pilot work in human fetal kidneys (16–19 weeks' gestation) established that the $T_2\beta$ antibody preparation was strongly and consistently expressed in formalin-fixed paraffin-embedded material as well as cryostat sections.

In the developing mesonephric kidney of the earliest embryos available, the most primitive caudal condensations of nephritic tissue are $T_2\beta$ immunonegative (Fig. 2A). As nephric vesicles develop progressively rostrally, weak focal $T_2\beta$ immunopositivity is present in some cells. With further development of the mesonephric kidney, which is present up to 9–10 weeks' gestation, mesonephric tubules, occasional cells of the parietal epithelium of Bowman's capsule and the mesonephric duct are $T_2\beta$ immunopositive with some glomerular cells weakly immunoreactive (Fig. 2B).

The ureteric bud arising from the mesonephric duct at 32 postovulatory days elongates to form the ureter and renal pelvis (Fig. 2C) and then sequentially divides into calyxes and collecting ducts of the developing metanephric kidney (Fig. 2D). In the ureteric bud derivatives, $T_2\beta$ immunostaining has a distinct caudal to rostral pattern of

reactivity. In embryos and fetuses up to 10 weeks' gestation the columnar epithelium of the pelvis (Fig. 2D) and ureter (Fig. 2E) are strongly $T_2\beta$ immunopositive, but this decreases through the length of the developing calyxes and collecting ducts such that the most rostral cells at the growing ends of the ducts are weakly $T_2\beta$ immunopositive (Fig. 2D). This caudal to rostral gradient of reactivity is still obvious in the collecting ducts and tubules until the end of the period of nephrogenesis at around 34–36 weeks' gestation. In embryos and early fetuses, the cellular distribution of $T_2\beta$ immunoreactivity in ureteric bud derivatives has no obvious pattern

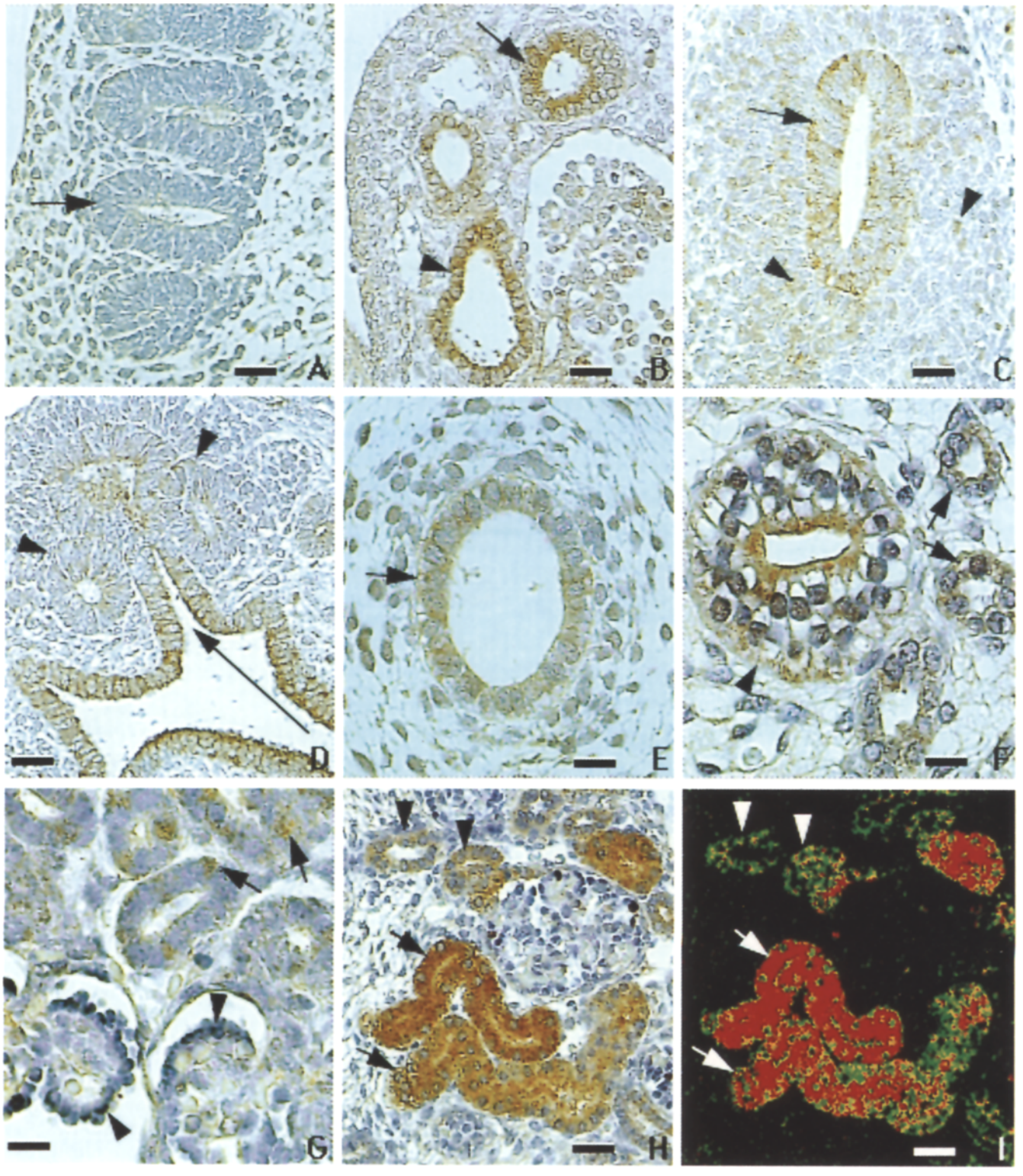

(Fig. 2C–E) but with further maturation and between 12 weeks' gestation and late fetal life immunoreactivity is displaced, predominantly to the apices of cells, by perinuclear glycogen deposits (Brigette Kaissling, personal communication), particularly obvious in collecting duct epithelium (Fig. 2F). The ureter and pelvis become $T_2\beta$ immunonegative with the development of an early transitional epithelium between 10 and 20 weeks' gestation. In the ureteric bud derivatives of late fetal kidney, $T_2\beta$ immunoreactivity is confined to the epithelium of renal papillae, ducts of Bellini and collecting ducts (Fig. 2F).

During the period of active nephrogenesis from 8 to 34 weeks' gestation the subcapsular cells and cellular masses which constitute the metanephric blastema are in general $T_2\beta$ immunonegative (Fig. 2D), although occasional cells are immunopositive (Fig. 2C). Renal vesicles and S-shaped bodies are immunonegative and only with the appearance of a primitive glomerulus do the corresponding tubules develop weak focal positivity in some cells (Fig. 2G). With further development, the developing proximal tubules become intensely $T_2\beta$ immunopositive (compare Fig. 1G and 1H from the same 16-week gestation fetal kidney). The parietal layer of Bowman's capsule is reactive at the urinary pole of the renal corpuscle (Fig. 2H). As nephrons elongate and differentiate from around 12 weeks' gestation, all segments (proximal, loop of Henle and distal tubule) retain $T_2\beta$ immunoreactivity with the most intensive staining in proximal tubules, where this has a widespread distribution within the cell (Fig. 2H,I). In addition, some glomerular cells adjacent to the urinary space are also reactive confirming that the podocytes of the visceral layer of Bowman's capsule are $T_2\beta$ immunopositive (Fig. 2H,I).

Fig. 2 Immunohistochemistry of T2β in: **A** a 32 postovulatory day embryo showing that developing renal vesicles in mesonephric kidney (*arrow*) are immunonegative, ×230; **B** a 56 postovulatory day embryo showing that reactivity is present in mesonephric tubules (*arrow*) and mesonephric duct (*arrowhead*), ×230; **C** a 37 postovulatory day embryo showing that the epithelium of the first division of the ureteric bud (*arrow*) is focally immunopositive and that some cells of the metanephric blastema are reactive (*arrowhead*), ×230; **D** a 10-week gestation fetal metanephric kidney showing that immunoreactivity is present in the ureteric bud derivatives and this decreases from central to peripheral (*arrow direction*) and that developing renal vesicles are immunonegative (*arrowheads*), ×230; **E** a 9-week gestation metanephric ureter showing immunoreactivity in the columnar lining cells (*arrow*), ×230; **F** a 19-week gestation fetal kidney showing that staining is predominantly displaced apically in collecting duct epithelium by perinuclear glycogen deposits (*arrowhead*) and that loops of Henle are less reactive (*arrows*), ×460; **G** the sub-nephrogenic zone of a 16-week gestation fetal kidney showing that cells in developing tubules are focally reactive (*arrows*) and developing glomeruli are immunonegative (*arrowheads*), ×460; **H** the inner cortical zone of a 16-week gestation fetal kidney (same as **G**) showing proximal tubules are intensely positive (*arrows*), distal tubules less reactive (*arrowheads*) and only occasional cells in the glomerulus are immunopositive, ×230; **I** false colour image of the intensity of $T_2\beta$ immunoreactivity in a 16-week gestation fetal kidney (same as **H**) showing that the most intense staining (*red*) is in proximal tubules (*arrows*) with lesser reactivity (*green*) in distal tubules (*arrowheads*), ×230. **A–E, H, I** *Bar*=50 μm, **F, G** *bar*=25 μm

Image analysis

Threshold settings R1B1G1 for false red and R2B2G2 for false green were selected using $T_2\beta$ immunostained proximal tubules which allows capture of approximately 90% of 3,3-diaminobenzidine staining in this the most intensely immunoreactive renal component, yet without significant background interference (Fig. 2H,I).

In the metanephric kidney before 8 weeks' gestation and the onset of nephrogenesis, all $T_2\beta$ immunostaining is confined to ureteric bud derivatives (Fig. 2D). The localisation of $T_2\beta$ immunostaining changes with development and analysis of individual serial image sections (100×572 pixels) collected sequentially across transverse sections from the hilum to the capsule of three fetal kidneys (16–20 weeks' gestation) shows that the majority of $T_2\beta$ immunostaining is confined to the cortical zone co-localising with proximal tubules, distal tubules and the developing glomerulo-tubular complexes of the nephro-

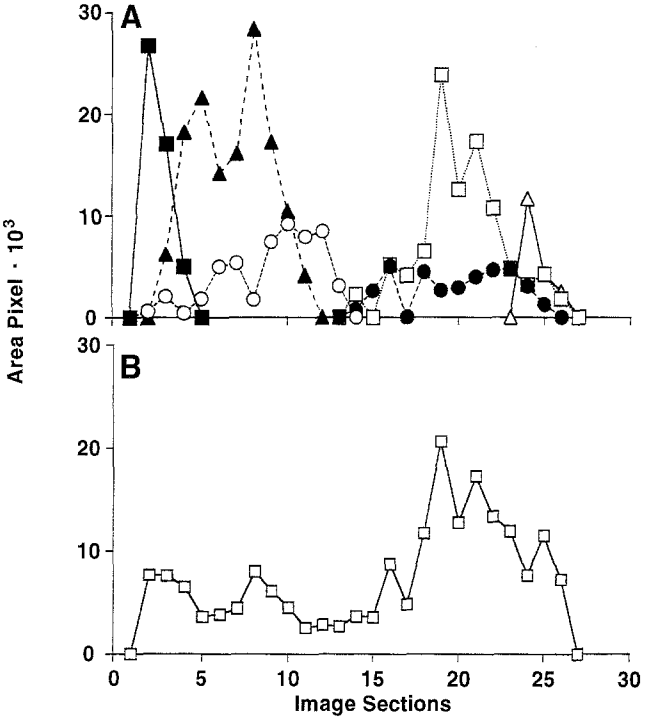

Fig. 3 **A** The epithelial areas (pixels) of renal components in a series of 100×570 pixel transverse image sections from the pelvis (section 0) to the capsule (section 27) in a 16-week gestation fetal kidney. Proximal tubules (39.8%; 1.0) □·····□; distal tubules (10.1%; 0.85) ●–·–●; primitive glomerulo-tubular complexes (1.4%; 0.22); loops of Henle (12.2%; 0.38) ○---○; collecting ducts (21.1%; 0.32) ▲---▲; papillary epithelium-ducts of Bellini (11.5%; 0.50) ■—■. The figures in parenthesis are (a) the percentage of total $T_2\beta$ epithelial immunoreactive area per renal component and (b) the ratio of $T_2\beta$ immunoreactive area: epithelial area of each component with proximal tubules as nominal value 1.0. **B** Summation of red and green threshold areas of $T_2\beta$ epithelial immunostaining (pixels) in the same series of 100×570 pixel image sections as **A** □—□. Variations in cortico-medullary thickness did not allow overlap of equivalent graphical data from two other fetal kidneys, but similar patterns of $T_2\beta$ immunoreactivity were observed

Table 1 Glucose-6-phosphatase activity in human fetal kidney microsomes. Data are mean±SEM (age range 15–25 weeks' gestation, n=10)

Substrate	Intact microsomes		Disrupted microsomes	
	V_{max} nmol/min/mg	K_m mM	V_{max} nmol/min/mg	K_m mM
Glucose-6-phosphate	20.4±5.6	3.9±0.6	21.7±4.5	1.4±0.3
Pyrophosphate	19.1±7.9	3.0±0.7	24.4±5.7	1.1±0.2

genic zone. Figure 3A shows the distribution of the epithelial areas of individual renal components and Fig. 3B the total immunostaining in the same series. The summation of the areas of $T_2\beta$ immunostaining, equivalent to the false red and green channels, for individual kidney components shows that proximal tubules contribute the greatest epithelial area of immunoreactivity (approximately 40%). However, surprisingly, around 45% of $T_2\beta$ immunostaining is present in the medulla, co-localising with the distribution of collecting ducts, loops of Henle and ducts of Bellini (Fig. 3A,B). This relatively high medullary percentage contribution to immunostaining is not obvious by visual inspection alone. The ratio of $T_2\beta$ immunoreactive area: epithelial area as a measure of the relative intensity of staining in each renal component, with proximal tubules having a nominal value of 1.0, is widely variable throughout the kidney parts (Fig. 3A,B). For example, although collecting ducts contribute around 21% of the total immunoreactivity they have a relative intensity of staining which is only one third that of proximal tubules (Fig. 3A,B).

Enzyme activities

Glucose-6-phosphatase activity in fully disrupted microsomes is a measure of the activity of the catalytic subunit of the glucose-6-phosphatase enzyme without the rate limitations imposed by the transport proteins. The levels of human fetal kidney glucose-6-phosphatase enzyme activity (V_{max}) with both glucose-6-phosphate and pyrophosphate as substrates were found to be very similar (Table 1) to those previously reported in human fetal liver [10] and are about 10% of the values previously reported in normal adult human liver (e.g. [10, 29]). The K_m of the human fetal kidney glucose-6-phosphatase enzyme is within the range of K_m values that we have previously found in both fetal and adult human liver glucose-6-phosphatase enzymes, mean 0.8 mM±0.04 (SEM) (n=222) [10].

Glucose-6-phosphatase activity in intact microsomal vesicles with glucose-6-phosphate as substrate is a measure of the combined rates of the glucose-6-phosphatase enzyme and its associated microsomal glucose-6-phosphate, phosphate and glucose transport proteins. The V_{max} of the glucose-6-phosphatase system in intact human fetal kidney microsomes with glucose-6-phosphate as substrate (Table 1) is very similar but slightly lower than the V_{max} in disrupted microsomes, the latency being 6%. This demonstrates that the transport proteins (for glucose-6-phosphate, phosphate and glucose) are all functional in fetal kidney microsomes.

Glucose-6-phosphatase activity in intact microsomes with pyrophosphate as substrate is a measure of the combined rates of the glucose-6-phosphate enzyme and the T_2 transport system for phosphate and pyrophosphate. The activity (V_{max}) with pyrophosphate as substrate was 22% latent with a K_m of 3.0 mM (Table 1) confirming that T_2 is present in human fetal kidney and that it has a similar K_m to that previously found in human liver [10, 26].

Discussion

A patent mesonephric duct and nephric tubules are present in human embryos from stage 12, 26 post-ovulatory days [28] and although glomerulo-tubular units are reabsorbed, rostral to caudal, in late embryonic-early fetal life, individual units are still present at 9–10 weeks' gestation, when glomeruli and tubules are beginning to appear in the developing metanephric kidney (Fig. 2D). The most rostral segments of the mesonephric duct and tubules are $T_2\beta$ immunopositive from as early as 32 post-ovulatory days and this spatial and temporal expression of the $T_2\beta$ protein is similar to that of the catalytic unit of the glucose-6-phosphatase system [21]. Derivatives of the ureteric bud, namely ureter, pelvis and calyces, are transiently $T_2\beta$ immunopositive in the early metanephric kidney, as is the catalytic unit of the glucose-6-phosphatase system [21].

Our studies show that in metanephric kidney, by mid-gestation, the proximal tubules contribute the greatest epithelial area of $T_2\beta$ immunoreactivity as well as intensity of immunostaining. In addition, we have shown that there are lesser degrees of $T_2\beta$ immunoreactivity, in terms of both area of contribution as well as intensity of staining, in other tubular components and collecting ducts. Overall, $T_2\beta$ immunoreactivity is greater in the cortex (mainly proximal and distal tubules) compared to medulla (predominantly loops of Henle and collecting ducts). However, the cellular and regional predominance of $T_2\beta$ immunoreactivity in the metanephric kidney changes with ontogeny. In embryos and early fetuses, the developing pelvis, calyxes and collecting ducts are the principal structures which are $T_2\beta$ immunopositive and only with the development of nephrons in later gestation does this early predominance of $T_2\beta$ immunoreactivity to ureteric bud derivatives change, such that by mid-gestation the reactivity in collecting ducts is a small propor-

tion of the total. These changes in spatial and temporal expression of the $T_2\beta$ protein are also similar to that of the catalytic unit of the glucose-6-phosphatase system [21].

The common spatial and temporal expression of both the $T_2\beta$ protein and the catalytic unit of the glucose-6-phosphatase system suggests that unlike human fetal liver [10], the kidney $T_2\beta$ protein is not developmentally delayed compared to the enzyme. Consistent with this is the low latency of glucose-6-phosphatase activity in intact human fetal kidney microsomes with pyrophosphate as substrate which shows that the level of T_2 transport capacity is appropriate for the amount of enzyme activity present (Table 1). This is in complete contrast to the high latency (up to 100%) of glucose-6-phosphatase activity in intact human fetal liver microsomes with pyrophosphate as substrate that we found previously in liver samples of the same gestational range [10, 26]. The earlier temporal expression of the endoplasmic reticulum pyrophosphate (and carbamyl phosphate) transport capacity in kidney compared to liver may reflect the importance of pyrophosphate and carbamyl phosphate as substrates in human fetal kidney.

Renal disease is a well-recognised late complication of type I glycogen storage disease commonly including focal segmental glomerulosclerosis, interstitial fibrosis, renal stones and nephrocalcinosis and more rarely amyloidosis, a Fanconi-like syndrome and distal renal tubular acidosis [13, 14]. The presentation of overt renal disease in type I glycogen storage disease occurs late in childhood or adulthood and children under 10 years of age usually have normal renal function [15], although provocative renal function tests may detect subtle changes [32]. The diagnosis of type I glycogen storage disease is usually made at 3–4 months postnatal age, although this may be delayed later into childhood, and no studies have answered the question at what age renal histological changes begin to appear in affected children [14]. In preterm infants, detection of subtle renal abnormalities is further complicated by the dysfunctions of immaturity and concurrent disease [27]. Our index case of a preterm infant, who was born at 30 weeks' gestation and died of cor pulmonale secondary to bronchopulmonary dysplasia (treated with furosemide) on postnatal day 182, had no T_2 pyrophosphate translocase function in both liver and kidney microsomes. Postmortem revealed normal gross structure and normal routine renal histology. A calculus 4 mm in diameter was found in a major calyx of the left kidney but with no evidence of nephrocalcinosis and although this is a commonly recognised complication of type I glycogen storage disease, it also occurs in some preterm infants treated with furosemide (e.g. [1]).

As our index case had no T_2 pyrophosphate translocase function in either liver or kidney microsomes, whereas our control samples of kidney had T_2 pyrophosphate transport capacity appropriate to their levels of enzyme, it is likely that it is either a genetic deficiency affecting both liver and kidney T_2, or, a developmental disorder originating prior to 15 weeks' gestation (the earliest time we measured T_2 function). These possibilities will only be distinguished when DNA probes for T_2 become available.

Acknowledgements This work was supported by grants from the National Kidney Research Fund (A.B., R.H.); Scottish Home and Health Department (A.B., R.H.); Wellcome Trust (R.H.); Tenovus (Scotland) (A.B., R.H.); A.B. was a Lister Institute Research Fellow.

References

1. Alon US, Scagliotti D, Garola RE (1994) Nephrocalcinosis and nephrolithiasis in infants with congestive cardiac failure treated with furosemide. J Pediatr 125: 149–151
2. Arion WJ, Ballas LM, Lange AJ, Wallin BK (1976) Microsomal membrane permeability and the hepatic glucose-6-phosphatase system. J Biol Chem 251: 4901–4907
3. Arion WJ, Lange AJ, Walls HE, Ballas LM (1980) Evidence for the participation of independent translocases for phosphate and glucose-6-phosphate in the microsomal glucose-6-phosphatase system. J Biol Chem 255: 10396–10406
4. Ashmore J, Weber G (1959) The role of hepatic glucose-6-phosphatase in the regulation of carbohydrate metabolism. Vitam Horm 17: 91–132
5. Bell JE, Hume R, Busuttil A, Burchell A (1993) Immunocytochemical detection of microsomal glucose-6-phosphatase in human brain astrocytes. Neuropathol Appl Neurobiol 19: 429–435
6. Burchell A (1992) The molecular basis of the type 1 glycogen storage diseases. Bioessays 14: 395–400
7. Burchell A, Cain DI (1985) Rat hepatic microsomal glucose-6-phosphatase protein levels are increased in streptozotocin-induced diabetes. Diabetologia 28: 852–856
8. Burchell A, Hume R, Burchell B (1988) A new microtechnique for the analysis of the human hepatic microsomal glucose-6-phosphatase system. Clin Chim Acta 173: 183–192
9. Burchell A, Gibb L, Waddell ID (1989) New microtechniques for the diagnosis of the type 1 glycogen storage diseases. In: Depuy C, Valette L (eds) Perinatal prevention of genomic anomalies. Foundation Marcel Merieux, Lyon, pp 96–103
10. Burchell A, Gibb L, Waddell ID, Giles M, Hume R (1990) The ontogeny of the human hepatic glucose-6-phosphatase proteins. Clin Chem 36: 1633–1637
11. Burchell A, Lyall H, Busuttil A, Bell J, Hume R (1992) Glucose metabolism and hypoglycaemia in SIDS. J Clin Pathol 45 [Suppl]: 39–45
12. Burchell A, Allan BB, Hume R (1994) The endoplasmic reticulum glucose-6-phosphatase proteins. Mol Membr Biol 11: 217–227
13. Chen Y-T (1991) Type I glycogen storage disease: kidney involvement, pathogenesis and its treatment. Pediatr Nephrol 5: 71–76
14. Chen Y-T, Burchell A (1995) Glycogen storage diseases. In: Scriver CR, Beaudet AL, Sly WS, Valle D (eds) The metabolic basis of inherited disease, chapter 24. McGraw-Hill, New York, pp 935–965
15. Chen Y-T, Coleman RA, Scheinman JI, Kolbede PC, Sidbury JB (1988) Renal disease in type I glycogen storage disease. N Engl J Med 318: 7–11
16. Colquhoun D (1971) Lectures on biostatistics. Clarendon Press, Oxford, pp 257–265
17. Cori GT, Cori CF (1952) Glucose-6-phosphatase of the liver in glycogen storage disease. J Biol Chem 199: 661–667
18. Fulceri R, Romani A, Pompella A, Benedetti A (1990) Glucose-6-phosphate stimulation of MgATP-dependent Ca^{2+} uptake by rat kidney microsomes. Biochim Biophys Acta 1022: 129–133
19. Hume R, Burchell A (1993) Abnormal expression of glucose-6-phosphatase in preterm infants. Arch Dis Child 68: 202–204

20. Hume R, Lyall H, Burchell A (1992) Impairment of the activity of the microsomal glucose-6-phosphatase system in premature infants. Acta Paediatr 81: 580–584
21. Hume R, Bell JE, Hallas A, Burchell A (1994) Immunohistochemical localisation of glucose-6-phosphatase in developing human kidney. Histochemistry 101: 413–417
22. Hume R, Voice M, Pazouki S, Giunti R, Benedetti A, Burchell A (1995) The human adrenal microsomal glucose-6-phosphatase system. J Clin Endocrinol Metab 80: 1960–1966
23. Lucius RW, Waddell ID, Burchell A, Nordlie RC (1993) The hepatic glucose-6-phosphatase system in Ehrlich-ascites-tumour-bearing mice. Biochem J 290: 907–911
24. Nordlie RC (1976) Glucose-6-phosphate phosphotransferase. In: Mehlman MA, Hanson RW (eds) Gluconeogenesis: its regulation in mammalian species. Wiley, New York, pp 93–152
25. Nordlie RC (1985) Fine tuning of blood glucose concentrations. Trends Biochem Sci 10: 70–78
26. Nordlie RC, Scott HM, Waddell ID, Hume R, Burchell A (1992) Analysis of human hepatic microsomal glucose-6-phosphatase in clinical conditions where the T2 pyrophosphate/phosphate transport protein is absent. Biochem J 281: 859–863
27. Oh W (1981) Renal functions and clinical disorders in the neonate. In: Lewy JE (ed) Symposium on perinatal nephrology. Saunders, Philadelphia, pp 215–223
28. O'Rahilly R, Muller F (1987) Developmental stages in human embryos. (Publication 637) Carnegie Institution of Washington, Washington, DC
29. Pears JS, Jung RT, Hopwood D, Waddell ID, Burchell A (1992) Ten cases of symptomatic adult hypoglycaemia due to hepatic glycogen metabolising abnormalities. Q J Med 299: 207–222
30. Peterson GL (1977) A simplification of the protein method of Lowry et al. which is more generally applicable. Anal Biochem 83: 346–356
31. Potter EL (1972) Normal and abnormal development in the kidney. Year Book Publishers, Chicago
32. Restaino I, Kaplan BS, Stanley C, Baker L (1993) Nephrolithiasis, hypocitraturia, and a distal renal tubular acidification defect in type I glycogen storage disease. J Pediatr 122: 392–396
33. Scammon RE, Calkins LA (1929) The development and growth of the external dimensions of the human body in the fetal period. University of Minnesota Press, Minneapolis
34. Sternberger LA, Hardy PH, Cuculis J, Meyer HG (1970) The unlabelled antibody method of immunohistochemistry: preparation and properties of soluble antigen – antibody complex (horseradish peroxidase-anti-horseradish peroxidase) and its use in identification of spirochaetes. J Histochem Cytochem 18: 315–333
35. Waddell ID, Lindsay JD, Burchell A (1988) The identification of T_2: the phosphate/pyrophosphate transport protein of the hepatic microsomal glucose-6-phosphatase system. FEBS Letts 229: 179–182